IET Generation, Transmission & Distribution

Research Article

Journals
The Institution of
Engineering and Technology

Dynamic equivalent of microgrid considering flexible components

ISSN 1751-8687
Received on 5th January 2015
Revised on 10th April 2015
Accepted on 3rd May 2015
doi: 10.1049/iet-gtd.2014.1237
www.ietdl.org

Jiacheng Hua[1] ✉, *Qian Ai*[1], *Yuan Yao*[2]

[1]*Department of Electrical Engineering, Shanghai Jiao Tong University, Shanghai 200240, People's Republic of China*
[2]*State Grid Suzhou Power Supply Company, Suzhou 215639, People's Republic of China*
✉ *E-mail: huajiacheng1990@126.com*

Abstract: Microgrid (MG) contains large scales of flexible components, so the traditional distribution network equivalent method is not applicable in MG equivalent research. In this study, a novel MG model structure considering the influence of control strategy on the external characteristics of MG is presented, in order to make measurement-based modelling approach more suitable for equivalent research of MG. The proposed model is a non-mechanism model which can restore the dynamic characteristics of MG better, and the parameters identification of the model is solved by improved immune algorithm. Finally, through the fault validation way the effectiveness of the model is demonstrated.

1 Introduction

Nowadays, large scales of renewable distributed generations (DGs) have been integrated into the power grid, which leads to the result that more and more flexible components appear in power system. The development of these components brings new problems to [illegible]

[illegible] Microgrid (MG) is an innovative way to integrate large amount of renewable DGs into distribution power system and make the power system more reliable and flexible [3, 4]. Most of the components in MG subject to the control strategy of the MG, whereas the traditional equivalent model of the distribution network, such as induction motor in parallel with static load, cannot restore MG dynamic characteristics well enough. It is highly necessary to develop a new equivalent method which is more suitable for MG.

The difficulty of MG equivalent research lies in the diversity of DGs and the alterability of DGs control methods. Milanovic and Mat Zali [5] and Resende and Peas Lopes [6] tell the history and development of system identification methods based on measurement and simulation responses. In traditional load modelling, the inverters are not a big concern, but their influence cannot be ignored when it comes to MG where lots of devices are connected through inverters. There are two main kinds of inverter models at present: the first one is to model the electro-magnetic transient processes of the power electronic devices in detail [7], which can express the accurate electro-magnetic process of the inverter; however, the model is quite complicated. The calculation speed will be extremely slow [8]. The second one is the quasi-steady-state model, which simplifies the inverter as a voltage source. This model can facilitate the analysis and calculation of MG, but omits the dynamic processes of the power electronic devices [9].

There are several references about the modelling of the control part of DG units. Katiraei and Iravani [10] consider the energy managements modelling and address real and reactive power management strategies of electronically interfaced DG in MG. It stated that based on the reactive power controls adopted, three power management strategies are identified and investigated. The real power of each DG unit is controlled based on frequency-droop characteristic. Katiraei *et al.* [11] investigate preplanned switching events and fault events that lead to islanding of a distribution subsystem and formation of a micro-grid. Moreover, the case study shows its feasibility. Katiraei *et al.* [12] represent a systematic approach to small-signal modelling of a micro-grid system in a rotating $dq0$ frame. Yazdani and Iravani [illegible]

[illegible] make sense in such system, measurement-based modelling approach turns to be a more efficient way in MG equivalent studies. In references [15, 16], the slow dynamics of MG is restored by a non-mechanism model, and its parameters are solved by PSO algorithm. Compared with non-mechanism model, mechanism model such as composite load model is more widely used in power system analysis software. Lei *et al.* [17] and Ju *et al.* [18] give the equivalent models of the inverter of different control methods in MG and load modelling and verify them. Anyhow, model structure is the key factor in MG equivalent study. It is known that the parameters of the components of certain condition are generally given by the manufacturer. However, the parameters of the MG as a whole are not clearly known. Parameter identification of MG is the base of control of MG. Mat Zali and Milanovic [19] present the development of the dynamic equivalent model of an active distributed network based on the grey-box approach. It can be referenced in MG modelling. Feng *et al.* [20] focus on deriving dynamic equivalents of distribution network taking distributed generators into consideration. It shows that the system identification method can be used into small group of grid. Papadopoulos *et al.* [21] show the increased complexity in predicting dynamic performance of MGs, and gives the road to overcome it.

On the basis of the analysis of the external dynamic characteristics of MG, this paper develops equivalent methods by measurement-based modelling approach. A major contribution is that a novel non-mechanism model structure considering the influence of control strategy on the external characteristics of MG is presented to make measurement-based modelling approach more suitable for equivalent research of MG, which can restore the dynamic characteristics of MG better. The parameters identification of the model is solved by improved immune algorithm. In Section 2, a simulation platform applying MATLAB/

SIMULINK is set up, and short-circuit fault is added to the system for MG dynamic characteristics observation. Section 3 discusses the principle of measurement-based modelling approach and the realisation of the identification algorithm. The model structure is performed in this section according to the control structure of MG. In Section 4, case study is performed and generalisation of the model and dispersion of parameters are discussed. Former research shows the method is suitable in asymmetrical fault situation [22]. The dynamic equivalent of MG introduced in this paper considers MG as an organic whole, and uses non-mechanism model to identify it. It is much faster to use the method introduced in this paper than the method of making equivalent of every component or mathematical deduction. The study in this paper lays a theoretical foundation of active distribution network voltage stability, multi-MG coordination control and MG behaviour pattern.

2 MG and its control strategy

2.1 Introduction of MG

MG is a new type of energy supply network and management structure, which can provide convenient renewable energy equipment access and realise demand side management. MG consists of various DGs, energy storages, loads and protection and control equipment, and can operate in either grid mode or islanded mode. Common DGs include photovoltaic (PV) cell, micro turbine (MT), wind generator and fuel cell (FC) [23]. The MG is centrally controlled and managed by an MG central controller installed at the MV/LV substation [24, 25].

2.2 Simulation of MG external characteristic under master–slave control strategy

The simulation system is shown in Fig. 1*a*. The single line diagram of the simulation system comprises the main grid which is a large power supply and the external distribution network (mainly consisting the distribution network load) connected to an MG with two inverter controlled DGs (PV and MT). The main grid (voltage level = 110 kV and $X/R = 10$) connects to the MG through a 110 kV/10 kV and 10 MVA transformer. Power rating of the DGs in the MG is $P_{\text{PVmodule}} = 6$ kW and $P_{\text{MT}} = 11$ kW. Here uses the detailed PV and MT modelling from Chapter 4 of reference [25]. The one-line diagram of PV and MT models is shown in Figs. 1*b* and *c*.

The case assumes that the MG initially run in netting state, where the active and reactive loads are mainly supplied by local DGs. When three-phase short-circuit fault occur in $t = 0.5$ s and recover in $t = 0.6$ s, the external characteristics of the system is shown in Figs. 1*d*–*g*. (power absorption is positive, else negative).

Observing the simulation curve, we find an obvious dynamic process of micro source even using constant power control. Therefore it is not strict to take micro source using constant power control as static load in transient analysis. The observed dynamic process is of tens of milliseconds level; the process cannot be ignored in some of the transient simulation case which requires high precision of dynamic process that leads to our study of dynamic equivalent of MG.

3 Modelling approach of MG equivalent

Traditional component-based modelling approach rarely makes sense in systems containing inverters, whereas MG contains large scales of inverters, which have an inconvenient influence on MG dynamic characteristics. This paper chooses measurement-based modelling approach, which can avoid physical modelling of

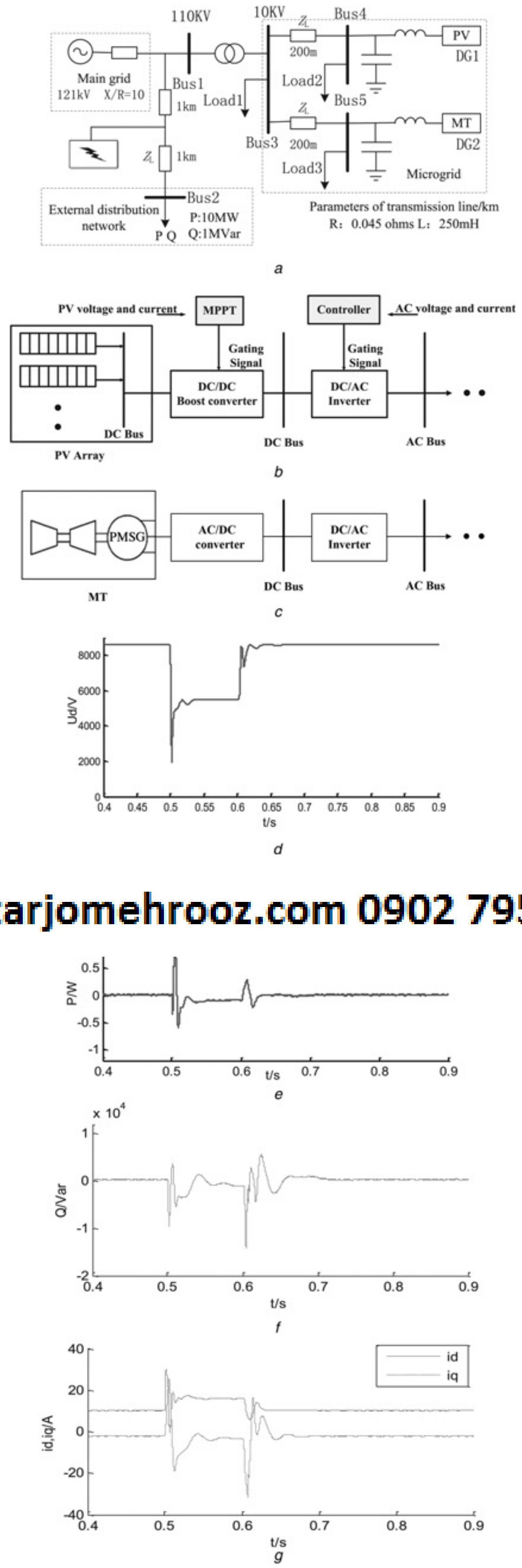

Fig. 1 *Simulation system and simulation curves of MG external characteristics*

a Simulation system
b One-line diagram of PV model
c One-line diagram of MT model
d 10 kV bus voltage curve
e 10 kV bus transmission active power
f 10 kV bus transmission reactive power
g DG1 *d*–*q*-axis current

inverters and translate control method of micro source through transfer functions.

3.1 Measurement-based modelling approach [26]

Measurement-based modelling approach is a typical problem of grey box, which knows the input and output data and the model structure of the system, to seek the optimisation of model parameters. The obtained model can restore the characteristics of the original system. Principle of measurement-based modelling approach is shown in Fig. 2 [27].

Parameter identification of measurement-based modelling approach is a process of solving optimisation problems, the objective function V_N of the problem is

$$\varepsilon(t|\theta) = y(t) - \hat{y}(t|\theta) \tag{1}$$

$$V_N = \sum_{t=1}^{N} \left\| \varepsilon(t|\theta) \right\|^2 \tag{2}$$

where $y(t)$ is the actual system output, $\hat{y}(t|\theta)$ is the model simulation output under currently identified parameters, $\delta(t)$ stands for the actual system disturbance. Then this paper chooses improved immune algorithm to do the parameter identification.

3.2 Improved immune algorithm

An improved immune algorithm named B-cell group evolvement-based immune algorithm (BGEIA) has been presented in the process of parameter identification. BGEIA consists of three relatively independent parts. They are quick searching in all the optimal solution, finding a new optimal solution neighbourhood and maintaining the diversity of B-cell populations. To optimise

distance from the immunoglobulin genes (V area), to realise the rapid optimisation of the optimal solution neighbourhood by the evolution of the B-cell groups, to find the new optimal solution neighbourhood by the replacement of the B-cell groups, to maintain the diversity of the B-cell groups so that the replacement of the B-cell groups is able to find the global optimum neighbourhood. The combination of the three makes the algorithm convergence to global optimal solution rapidly [28].

The flowchart of the BGEIA is shown as follows Fig. 3.

Basic procedure is illustrated as follows [29]:

Step 1: Initially use the immune cells generated by the parameters of immune algorithm to create populations of certain size randomly, and then divide them into some niches.
Step 2: Let immune cells optimise in the niche (cross-over or variation).
Step 3: Select the optimal immune cells within each niche for cross-over or mutate.
Step 4: Exit the programme when the affinity meets a certain value. Thus, the optimal immune cells in the population are the optimal parameters. Otherwise, go to step 2.

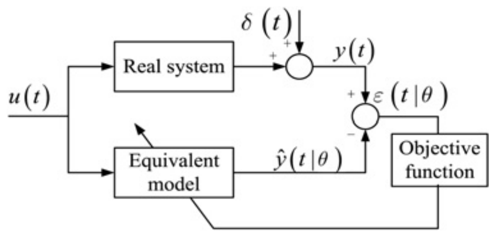

Fig. 2 *Principle of measurement-based modelling approach*

Then the idea to use improved immune algorithm BGEIA into practical MG model parameters optimised recognition is to take the parameters to be identified as antigens, and to take the objective function showed in (3) as antibody, the purpose is to seek a set of optimal load model parameters to obtain the best affinity of the antibody and antigen

$$J = \sqrt{\sum_{k=1}^{n} \left(\left(\frac{P(k) - P_r(k)}{P_r(k)} \right)^2 + \left(\frac{Q(k) - Q_r(k)}{Q_r(k)} \right)^2 \right)} \tag{3}$$

In the above equation, n is the number of data points, P and Q are the powers of the load model, P_r and Q_r are the actual measurements of the power.

Traditional immune algorithm has the disadvantages of high calculation price, slow convergence speed, and when the immune algorithm searches near optimal solution it cannot accurately determine the position of the optimal solution. Moreover, immune algorithm has premature phenomenon in the evolution. To improve the performance of the immune algorithm to solve practical problems and overcome the shortcoming of immune algorithm, improved immune algorithm BGEIA is used in this paper to identify external characteristic parameters. Improved immune algorithm BGEIA has been applied in the field of electric power system optimisation and load modelling [22, 30]. Compared with other parameter identification methods, BGEIA has distinct advantages. Its optimisation performance and robustness are strong. It has good parallelism, feasibility and simplicity. This algorithm can make the relationship between the global search and local search not only relatively independent, but also mutual assistance to complete the mission of the global search. This can make the algorithm search in the whole solution space find out more potential best individual, and avoid high fitness individual

Schwefel (f3), Shubert (f4) and Shaffer (f5) as test functions to compare the performance of PSO, GA and BGEIA. The average running time, average optimal value and standard deviation of these three optimisation algorithms are listed in Table 1.

Although PSO's speed is fast, it has the risk of dropping in local optimum. From Table 1, it can be seen that PSO's precision is not as good as BGEIA and GA. GA's precision is quite good to some test function; however, its running time is longer than that of other two

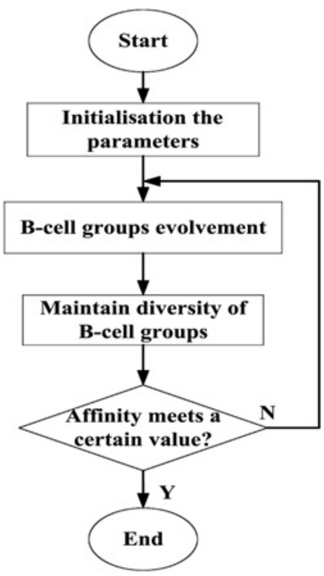

Fig. 3 *Flowchart of the BGEIA*

Table 1 Comparison of the average running time, average optimal value and standard deviation of three algorithms

Function		PSO	GA	BGEIA	Extreme value in theory
f1	average running time/s	0.185	0.395	0.199	0
	average optimal value	0.0049	0.0125	0.002	
	standard deviation	0.0071	0.0188	0.0035	
f2	average running time/s	0.166	0.501	0.23	0
	average optimal value	7.38×10^{-7}	0.162	7.85×10^{-9}	
	standard deviation	1.07×10^{-6}	0.5932	8.19×10^{-9}	
f3	average running time/s	0.164	0.487	0.226	−837.9
	average optimal value	−822.55	−837.96	−834.53	
	standard deviation	42.7	0	20.47	
f4	average running time/s	0.194	0.508	0.398	−186.7
	average optimal value	−180.28	−181.5	−184.74	
	standard deviation	11.43	10.85	3.88	
f5	average running time/s	0.156	0.465	0.271	0
	average optimal value	0.006	0.016	0.002	
	standard deviation	0.007	0.034	0.003	

algorithms. BGEIA has the best effect in overall optimisation and performs well in the aspect of speed.

From Fig. 4, the conclusion can be achieved that BGEIA can

chosen to solve the dynamic equivalent of MG.

3.3 Mathematical model of the control model structure

Constant PQ control, constant V/f control and droop control are the common control structures in MG to make micro source follow the preset value or work method. Generally speaking, to dual-loop controlled inverter, the outside loop reflects different control purposes, and the inside loop is used to fine adjustment, in order to improve the power quality of the inverter's output.

Control methods are reflected by the outside loop of the dual-loop controlled inverter. The frameworks of three control model structures' outside loop are shown in Figs. 5*a–c*.

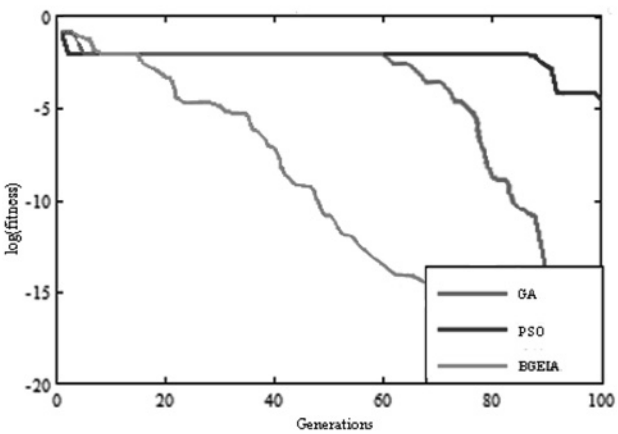

Fig. 4 *Curves comparison of fitness value of three*

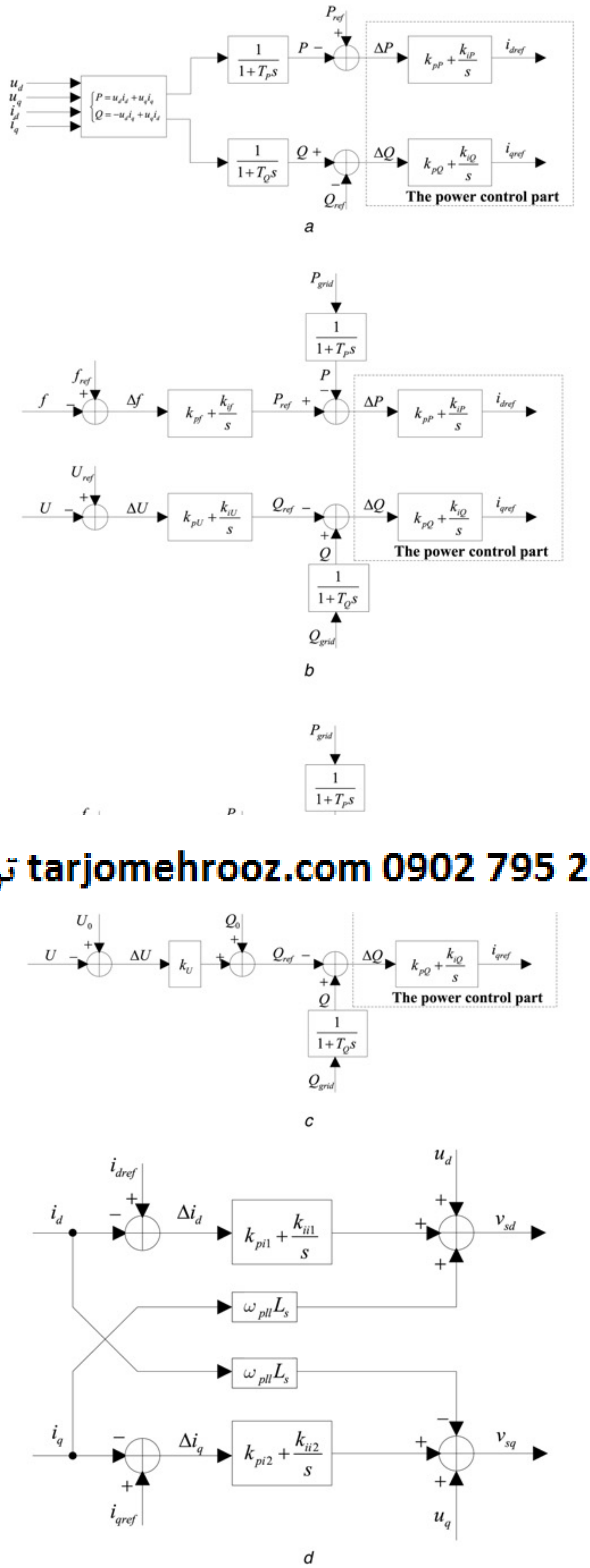

Fig. 5 *Frameworks of three control model structures*

a Framework of constant PQ control's outside loop
b Framework of outside loop of constant V/f control's outside loop
c Framework of droop control's outside loop
d Framework of three control models' inside current control loop

It can be concluded from Figs. 5*a* to *c* that the power control parts (in dotted box) of the three control structures' outside loop are the same. Therefore whatever the control structure is, the mathematical model of outside loop can be described by one equation. The mathematical model of outside power control loop is shown in (4)

$$\begin{cases} i_{\text{dref}} = \left(k_{pP} + \dfrac{k_{iP}}{s}\right)(P_{\text{ref}} - P) \\ i_{\text{qref}} = \left(k_{pQ} + \dfrac{k_{iQ}}{s}\right)(Q - Q_{\text{ref}}) \end{cases} \tag{4}$$

where P_{ref} and Q_{ref} are active and reactive power reference values, k_{pP} and k_{iP} are proportion and integration coefficients of the active power control and k_{pQ} and k_{iQ} are proportion and integration coefficients of the reactive power control.

The inside current control loop mainly adjusts the current to improve the power quality of the output and the system performance. Its dynamic response is quite quick. Here the inside loop uses *dq*0 coordinate system. The control model is shown in Fig. 5*d*, where i_d, i_q are the inverter output current *d*, *q* component, v_{sd}, v_{sq} are the inverter output voltage *d*, *q* component, u_d, u_q are the PCC voltage *d*, *q* component and L_s is the inductance of equivalent connecting reactor including filter circuit's inductance.

The mathematical model of inside current control loop is shown in (5)

$$\begin{cases} v_{sd} = \left(k_{pi1} + \dfrac{k_{ii1}}{s}\right)(i_{\text{dref}} - i_d) + \omega_{\text{pll}} L_s i_q + v_d \\ v_{sq} = \left(k_{pi2} + \dfrac{k_{ii2}}{s}\right)(i_{\text{qref}} - i_q) - \omega_{\text{pll}} L_s i_d + v_q \end{cases} \tag{5}$$

where $i_{d\text{ref}}$ and $i_{q\text{ref}}$ are direct and quadrature axes current reference values, v_{sd} and v_{sq} are output voltages of controlled voltage sources, L_S is the filter inductance, v_d, v_q, i_d and i_q are the filtered

Filter circuit equation is shown in (6)

$$\begin{cases} v_{sd} = L_s s i_d + \omega_{\text{pll}} L_s i_q + v_d \\ v_{sq} = L_s s i_q - \omega_{\text{pll}} L_s i_d + v_q \end{cases} \tag{6}$$

where L_S is the filter inductance, ω_{pll} is the system angular frequency measured by phase-locked loop.

Equation (7) is obtained after combining (5) and (6)

$$\begin{cases} L_s s i_d = \left(k_{pi1} + \dfrac{k_{ii1}}{s}\right)(i_{d\text{ref}} - i_d) \\ L_s s i_q = \left(k_{pi2} + \dfrac{k_{ii2}}{s}\right)(i_{q\text{ref}} - i_q) \end{cases} \tag{7}$$

Substitute (4) into (7)

$$\begin{cases} i_d = \dfrac{1}{sL_s}\left(k_{pi1} + \dfrac{k_{ii1}}{s}\right)\left[\left(k_{pP} + \dfrac{k_{iP}}{s}\right)(P_{\text{ref}} - P) - i_d\right] \\ i_q = \dfrac{1}{sL_s}\left(k_{pi2} + \dfrac{k_{ii2}}{s}\right)\left[\left(k_{pQ} + \dfrac{k_{iQ}}{s}\right)(Q - Q_{\text{ref}}) - i_q\right] \end{cases} \tag{8}$$

Build up the relationship between power and ac voltage by (9)

$$\begin{cases} P = u_d i_d + u_q i_q \\ Q = -u_d i_q + u_q i_d \end{cases} \tag{9}$$

Neglect the integral of inside loop because it has very fast dynamic response which has little concern with MG transient characteristics. Moreover, thus achieve the purpose of system order reduction which can reduce the difficulty of the identification as well. The transfer function equation is obtained after rewriting (7) as shown in (10)

$$\begin{cases} \Delta i_d(s) = \dfrac{Bs^2 + Cs + D}{s^2 + As}\Delta P(s) \\ \Delta i_q(s) = \dfrac{Fs^2 + Gs + H}{s^2 + Es}\Delta Q(s) \end{cases} \tag{10}$$

the analytic function of inside and outside control loop parameters and filter circuit parameters.

Fig. 6 shows the equivalent results for one DG (PV) with three different control strategies. ('Measured' data means the data are

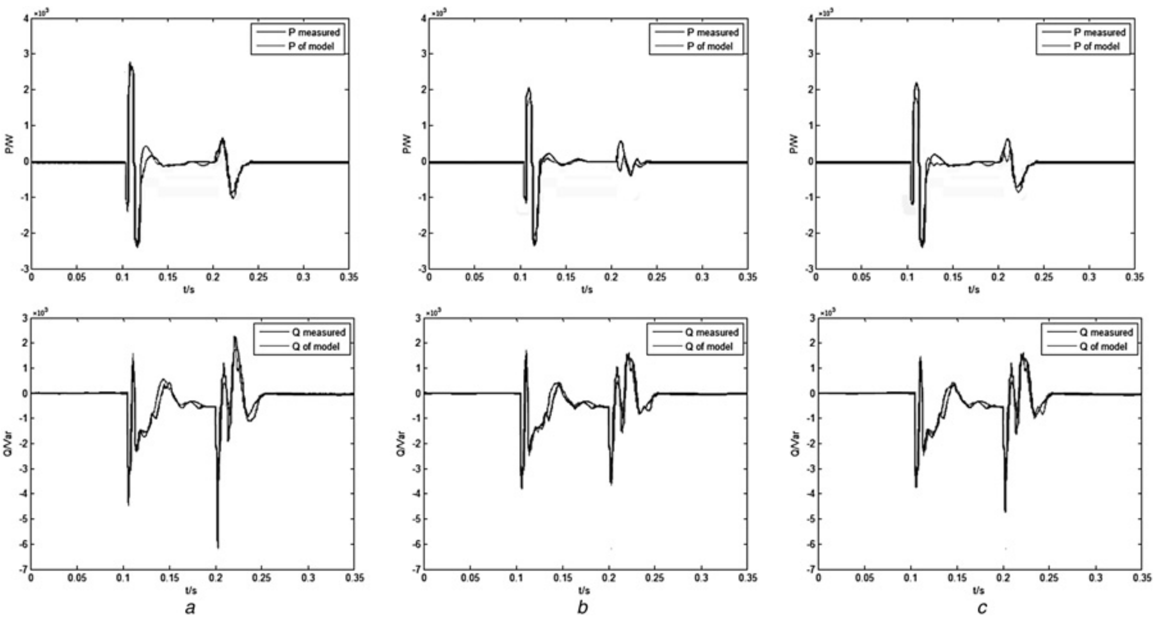

Fig. 6 *Equivalent results of one DG with different control strategies*

a One DG(PV) with PQ control strategy
b One DG(PV) with droop control strategy
c One DG(PV) with V/f control strategy

obtained from detailed simulation of the system in MATLAB/SIMULINK platform.) The results show that the dynamic equivalent method and model proposed in this paper have good effect on three control strategies on one DG.

4 Case study

4.1 Model identification results

Here studies the MG case represented in Fig. 1*a* to prove the approach proposed in this paper. The result is shown in Figs. 7*a* and *b*. The comparison of model output data and the source data in transient time scale are as follows in Figs. 7*c* and *d*. (‘Measured’ data means the data are obtained from detailed simulation of the system in MATLAB/SIMULINK platform.)

The identification algorithm BGEIA uses mean square error as the target function. There should be another index to evaluate its effect. Coefficient of determination R^2 to is used to quantify how well the fitting of parameters performs. We use function regress() in MATLAB to calculate coefficient of determination R^2. In this case, R^2 of active power is 0.9686 and R^2 of reactive power is 0.8647. They are both close to 1. This shows that the equivalent method and the fitting of parameters perform well.

4.2 Model generalisation

4.2.1 Interpolation and extrapolation capacities in different amplitude perturbations: Compare the simulation curves with model response curves in different amplitude perturbations (20 and 60% voltage drop in experimental conditions) to verify the interpolation and extrapolation capacities of model (identified by sample with a 40% voltage drop). The results are shown in Fig. 8.

According to fitted curves, despite the large difference in voltage

The model of this paper is built up by transfer functions and steady-state equations after the Park transformation, so it can apply to asymmetric disturbance situation theoretically [30], for what this paper verifies. Change the short-circuit type into *A*, *B* phase fault in simulation system. Verify the model in the dynamic process presented from the asymmetric fault, as shown in the Fig. 9 (here should consider *q*-axis voltage component).

4.3 Dispersion of model parameters

Identify the parameters of three different short-circuit fault samples whose durations are 0.1 s, ground resistances are 0.002, 0.001, 0.0006 and 0.0003 Ω, respectively. The corresponding voltage drops of four are 20, 40, 60 and 90% (in experimental conditions). The parameter identification results are shown in Table 2 (parameters A–H).

According to the table above, there exists dispersion in certain parameters, but within an acceptable range. The model structure and identification algorithm keep the identification results quite stable. The differences of eight parameters in 90% voltage drop and 40% voltage drop are very close. Only the parameter *B*’s difference is bigger.

This section presents the model identification results, and makes a comparison of model output and the source data in transient time scale. The results show that the model has good self-adaptability. Model generalisation ability is another emphasis discussed in this section. Model performance is observed in different amplitudes and types of faults or disturbances. The results presented in Fig. 9 show that the model has good generalisation ability in either symmetric or asymmetric disturbance situation. Moreover through the result shown in Table 2, we can draw the conclusion that the model parameters dispersion is acceptable on the premise of using improved immune algorithm.

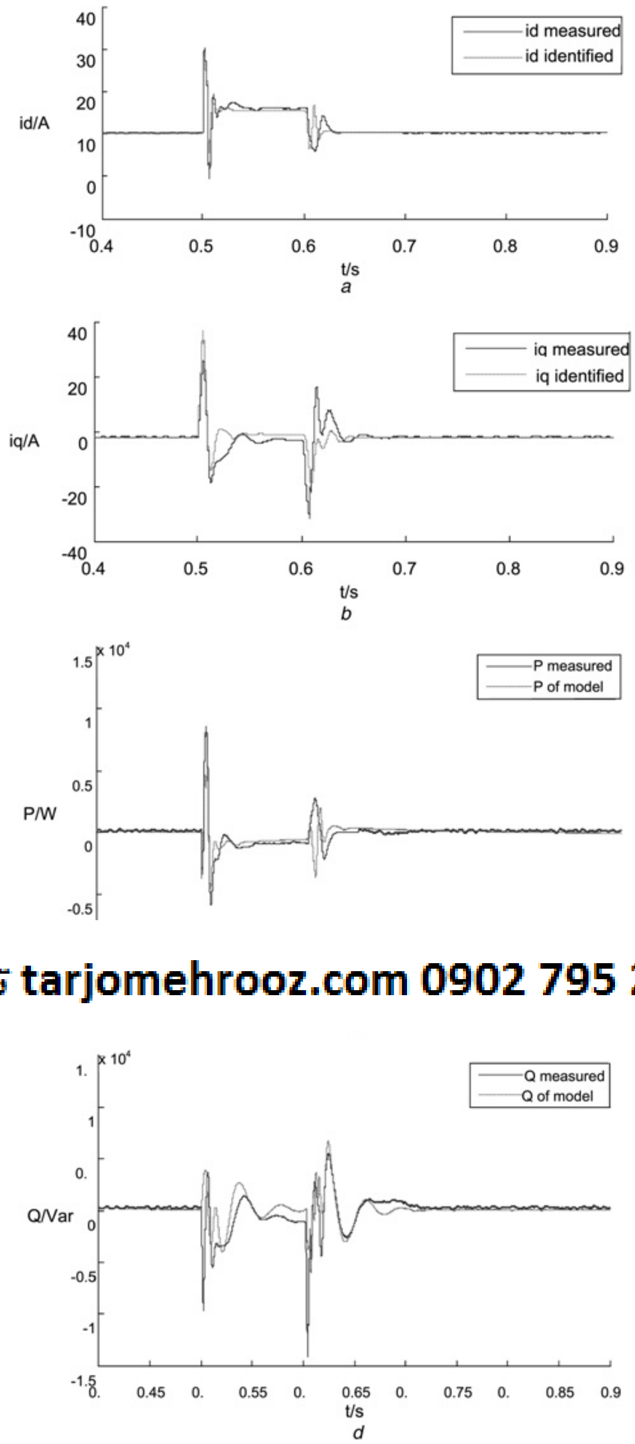

Fig. 7 *Equivalent results of MG*

a d-Axis current identification result
b q-Axis current identification result
c Fitted curve of active power
d Fitted curve of reactive power

4.4 Application in benchmark test

The model of this paper is tested on an MG benchmark. CIGRE 6 has given a medium voltage reference MG system (20 kV and 50 Hz) and Chen and Zhu [31] simplifies it as a modified MG test benchmark. The simplified CIGRE 6 MG benchmark is given in Fig. 10*a*. Here, the MVDC coupler is kept open and the left side subsystem 1 is mainly studied. The subsystem 1 in Fig. 10*a* is modified to an 8-Bus MG which is suitable for dynamic simulation and calculation as a benchmark test. The modified test MG benchmark which is

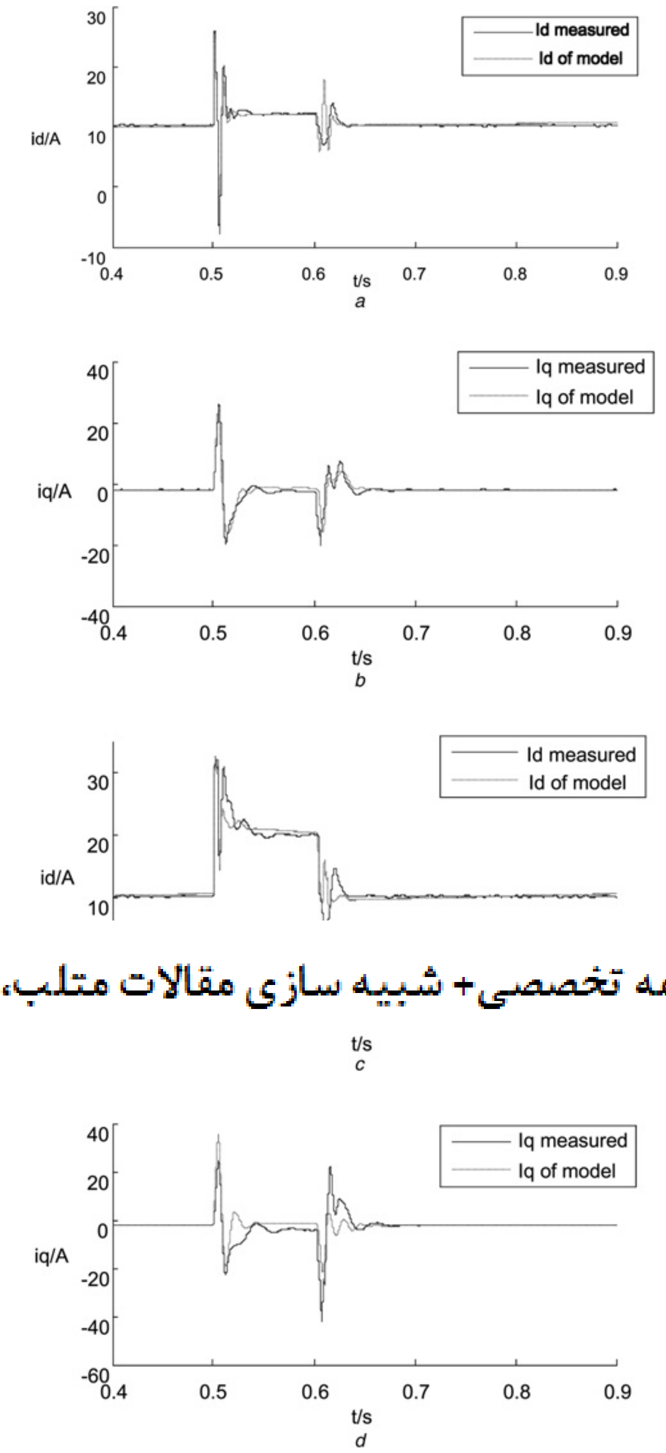

Fig. 8 *Verification of model interpolation and extrapolation abilities*

a d-axis current interpolation capacity (20% voltage drop)
b q-axis current interpolation capacity (20% voltage drop)
c d-axis current extrapolation capacity (60% voltage drop)
d d-axis current extrapolation capacity (60% voltage drop)

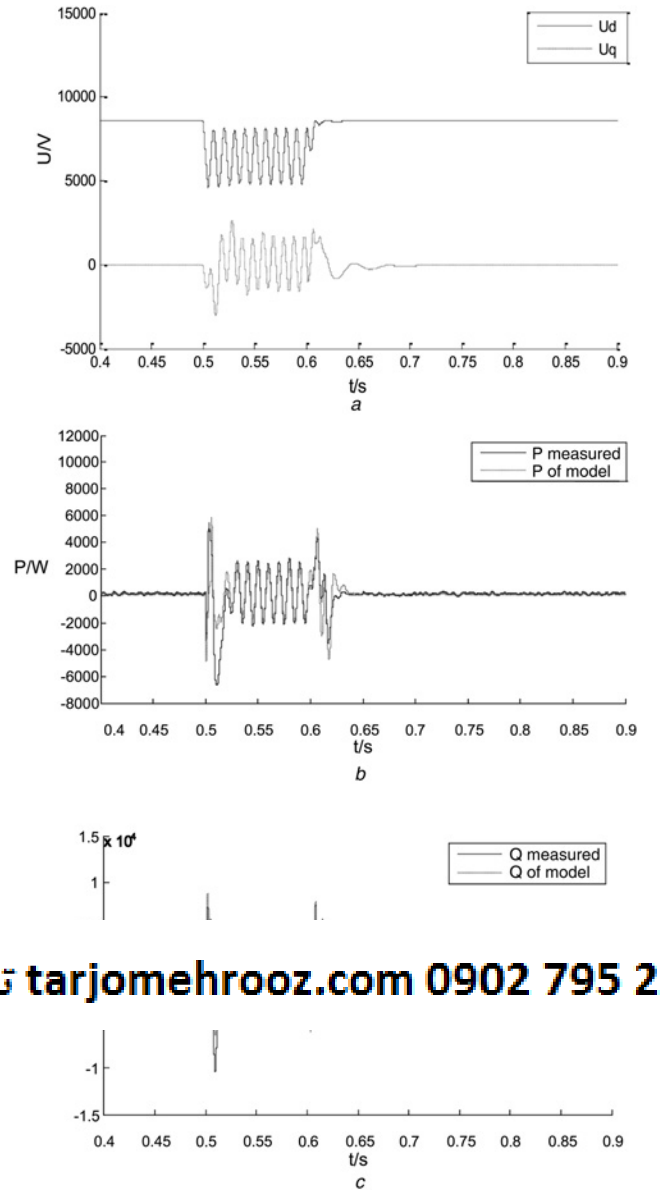

Fig. 9 *Results of model validation*

a Disturbance voltage in phase fault
b Active power calibration curve
c Reactive power calibration curve

studying in this paper is shown in Fig. 10*b*. The studying part (MG benchmark) of the system is represented using the proposed modelling method. The parameters are listed in Table 3.

Assume that the MG initially run in netting state, where the active and reactive loads are mainly supplied by local DGs. When three-phase short-circuit fault occur in $t = 0.6$ s and recover in $t = 0.71$ s. The comparison of model output data and the source data of the 8-Bus MG in transient time scale are as follows in Fig. 11.

R^2 of i_d is 0.942 and R^2 of i_q is 0.8529. The benchmark test result shows that the dynamic equivalent method proposed in this paper has a quite good effect in dynamic equivalent of MG. We can also find from coefficient of determination that in these cases the difference in the reactive power part is larger than the one in active power. Maybe simplification of neglecting the integral of inside loop in the model influences more on the reactive power part.

Table 2 Parameter identification results of three samples

	A	*B*	*C*	*D*
20%	−0.9104	−0.1037	0.3395	−0.0195
40%	−0.9233	−0.2405	0.4026	−0.0237
60%	−0.8978	−0.1125	0.5357	−0.0186
90%	−0.8722	−0.1191	0.5179	−0.0167

	E	*F*	*G*	*H*
20%	−0.9856	−0.07343	0.1409	−0.06733
40%	−0.9774	−0.08714	0.0833	−0.09644
60%	−0.9793	−0.08053	0.2584	−0.08467
90%	−0.9715	−0.07293	0.1549	−0.08935

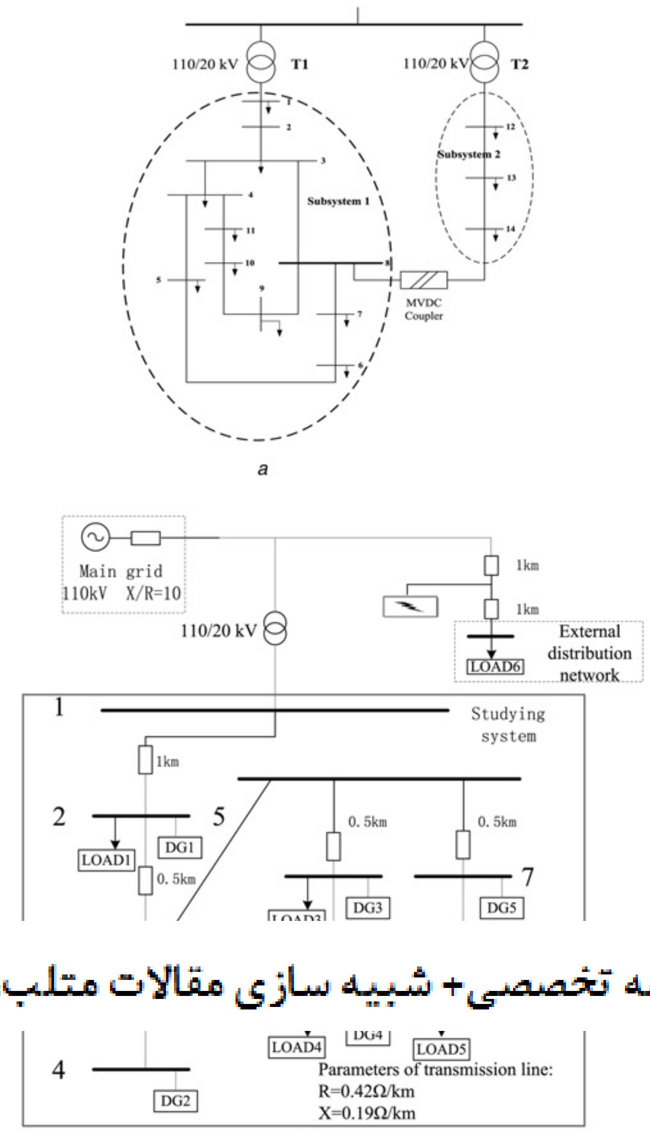

Fig. 10 *Test benchmark*

a Simplified CIGRE 6 middle-voltage benchmark system
b 8-Bus MG benchmark used in this paper derived from CIGRE 6 reference system

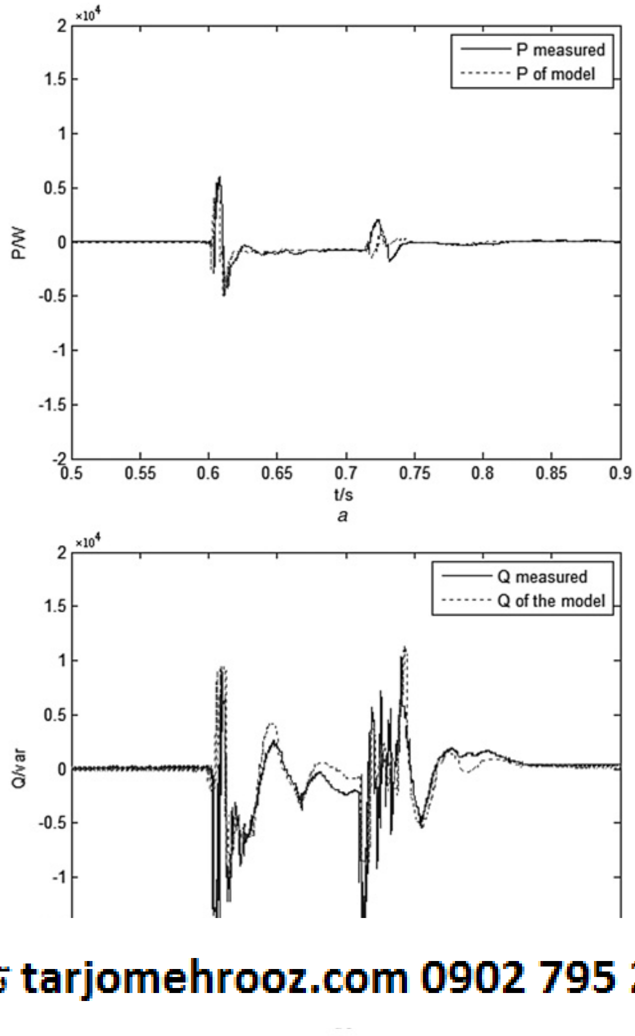

Fig. 11 *Equivalent results of the benchmark MG*

a Fitted curve of active power
b Fitted curve of reactive power

4.5 Application in MG clustering analysis

This section makes a case study to prove the availability of the method proposed in this paper in terms of clustering analysis based on external characteristic parameters. Self-adaptive FCM clustering algorithm is used here for MG clustering. Owing to the limitation of length of paper, self-adaptive FCM clustering algorithm theory is not explained here. It can be detailedly obtained from related reference.

The MG case's structure is just the same as the one in Fig. 1*a*. Table 4 lists six MG samples in the structure of Fig. 1*a*. Their components are different and can be divided into three real categories.

Then, we obtain six MG samples' identification parameters A–H, by applying dynamic equivalence method proposed in this paper. The identification parameters results are listed in Table 5.

Table 3 Parameter of the benchmark

DG	Type	Control strategy	P/MVA	Q/M_{var}
DG1	battery	constant PQ	0.35	0
DG2	PV	constant PQ	0.05	0
DG3	FC	droop	1	0.5
DG4	wind turbine	constant PQ	2	0
DG5	MT	constant V/f	3	0.8
LOAD		**P/MVA**		Q/M_{var}
LOAD1		0.7		0.06
LOAD2		0.5		0.05
LOAD3		0.9		0.1
LOAD4		0.7		0.06
LOAD5		1.2		0.08
LOAD6		10		1

Table 4 Six MG samples

MG no.	Components in MG	Fault type	Real category
1	PV module 5.4 kVA +100% motor	voltage drop (50%)	I
2	PV module 5.4 kVA +100% motor	voltage drop (90%)	I
3	PV module 5.4 kVA +50% motor+50% static load	voltage drop (50%)	II
4	PV module 5.4 kVA +50% motor+50% static load	voltage drop (90%)	II
5	PV module 5.4 kVA +100% static load	voltage drop (50%)	III
6	PV module 5.4 kVA +100% static load	voltage drop (90%)	III

Table 5 Identification parameters of six MG samples

MG no.	*A*	*B*	*C*	*D*	*E*	*F*	*G*	*H*
1	−1.3488	−0.08232	0.3721	−0.01898	−0.7866	−0.08234	0.2243	−0.1323
2	−1.5494	−0.05172	0.4377	−0.01583	−0.8672	−0.09299	0.1309	−0.1124
3	−0.9141	−0.1347	0.4021	−0.01891	−0.9774	−0.08733	0.1079	−0.07622
4	−0.8915	−0.1424	0.4329	−0.03945	−0.9479	−0.08296	0.1032	−0.09775
5	−0.7752	−0.1329	0.4871	−0.05889	−1.3223	−0.07742	0.09832	−0.07631
6	−0.7252	−0.1419	0.4794	−0.05177	−1.0121	−0.08209	0.06527	−0.09847

Table 6 Membership degree of six MG samples to three centres

MG no.	Membership degree to centre 1	Membership degree to centre 2	Membership degree to centre 3
1	0.882282	0.013638	0.104081
2	0.942167	0.010223	0.047611
3	0.014698	0.005019	0.980283
4	0.019662	0.006602	0.973736
5	0.080823	0.62983	0.289347
6	0.011204	0.966583	0.022213

After standardising the parameters and calculation analysis, vectors used in self-adaptive FCM clustering algorithm are formed. Adaptive efficiency coefficient $L(2, 3, 4) = (23.9281, 30.4865, 29.6862)$. It obtains its maximum value in $L(3)$. Therefore the optimal clustering number C is 3. Membership degrees of six MG samples to three centres are listed in Table 6.

According to the membership degree in Table 6, the conclusion is that MG samples 1 and 2 can be divided into one class, MG samples 3 and 4 can be divided into one class and that MG samples 5 and 6 can be divided into one class. The clustering result is the same as real category, so the clustering result is quite correct. The result proves the correctness and practicability of the dynamic equivalent method introduced in this paper from another aspect.

This paper studies the main problems of MG equivalent, including selection of equivalent methods, parameter identification method, selection of model structure and so on. The research starts with MG control strategy since it has significant influence on MG dynamic characteristics. Case study is performed to verify the effectiveness of the model. The non-mechanism model proposed in this paper provides a good revivification of MG dynamic characteristics, and it has good generalisation in different amplitudes or types of disturbances. The obtained model can be applied to short-term voltage stability and transient stability simulation analysis of multi-MG or grid containing MG.

The switching of MG control strategy will affect MG dynamic characteristics, which means the equivalent of MG should make better use of online operation information. The approach introduced in this paper can help build up equivalent model database by offline experiments. The combination of the database and online operation information constitutes the online modelling approach of MG which can be a fruitful area for further investigations.

6 Acknowledgments

The work is supported by the National Science and Technology Support Plan (2013BAA01B04) and State Grid Corporation of Science and Technology Projects (520940120036).

7 References

1 Wang, J.-L., He, R.-M., Ma, J.: 'Load modeling considering distributed generation'. Proc. Power Tech, IEEE Lausanne, 2007, pp. 1072–1077

2 Keyhani, A.: 'Modeling of photovoltaic microgrids for bulk power grid studies'. Power and Energy Society General Meeting, 2011, pp. 1–6

3 Lasseter, R.H.: 'Microgrids'. Power Engineering Society Winter Meeting, 2002, pp. 305–308

4 Hatziargyriou, N., Asano, H., Iravani, R., *et al.*: 'Microgrids', *IEEE Power Energy Mag.*, 2007, **6**, (3), pp. 78–94

5 Milanovic, J., Mat Zali, S.: 'Validation of equivalent dynamic model of active distribution network cell', *IEEE Trans. Power Syst.*, 2013, **28**, (3), pp. 2101–2110

6 Resende, F.O., Peas Lopes, J.: 'Development of dynamic equivalents for microgrids using system identification theory'. Proc. IEEE Lausanne Power Tech Conf., 2007, pp. 1033–1038

7 Shi, S.-S., Lu, Z.-X., Min, Y.: 'Verification of the equivalent model of the inverter in microgrid'. Proc. IEEE Int. Symp. on Power Electronics for Distributed Generation Systems, 2010, pp. 691–695

8 Zhou, M.-B., Qu, W.-L.: 'Power electronic technologies' (China Machine Press, Beijing, 2001)

9 Cheng, Y., Sun, Y.-J.: 'Summary of power electronic converter modeling', *Electr. Drive Autom.*, 2008, **30**, (6), pp. 4–9

10 Katiraei, F., Iravani, M.R.: 'Power management strategies for a Microgrid with multiple distributed generation units', *IEEE Trans. Power Syst.*, 2006, **21**, (4), pp. 1821–1831

11 Katiraei, F., Iravani, M.R., Lehn, P.W.: 'Micro-grid autonomous operation during and subsequent to islanding process', *IEEE Trans. Power Deliv.*, 2005, **20**, (1), pp. 248–257

12 Katiraei, F., Iravani, M.R., Lehn, P.W.: 'Small-signal dynamic model of a micro-grid including conventional and electronically interfaced distributed resources', *IET Gener. Transm. Distrib.*, 2007, **1**, (3), pp. 369–378

13 Yazdani, A., Iravani, R.: 'Voltage-sourced converters in power systems' (Wiley, Hoboken, NJ, 2010)

14 Milanovic, J.V., Kayikci, M.: 'Transient responses of distribution network cell with renewable generation'. PSCE'06, Atlanta, 2006, pp. 1919–1925

measurement data', *IET Gener. Transm. Distrib.*, 2014, **8**, (5), pp. 851–861

17 Lei, Q., Peng, F.Z., Yang, S.: 'Multiloop control method for high-performance microgrid inverter through load voltage and current decoupling with only output voltage feedback', *IEEE Trans. Power Electron.*, 2011, **26**, (3), pp. 953–960

18 Ju, P., Cai, C.-C., Cao, X.-Q.: 'General microgrid model based on physical background', *Proc. Electr. Power Autom. Equip.*, 2010, **30**, (3), pp. 7–14

19 Mat Zali, S., Milanovic, J.V.: 'Generic model of active distribution network for large power system stability studies', *IEEE Trans. Power Syst.*, 2013, **28**, (3), pp. 3126–3133

20 Feng, X., Lubosny, Z., Bialek, J.: 'Dynamic equivalencing of distribution network with high penetration of distributed generation'. Proc. of the 41st Int. Universities Power Engineering Conf., 2006. UPEC'06, 6–8 September 2006, pp. 467–471

21 Papadopoulos, P.N., Papadopoulos, T.A., Crolla, P., Roscoe, A.J., Papagiannis, G. K., Burt, G.M.: 'Measurement-based analysis of the dynamic performance of microgrids using system identification techniques', *IET Gener. Transm. Distrib.*, 2014, **9**, (1), pp. 90–103, 1

22 Xu, W.-H., Chen, C., Ai, Q., *et al.*: 'Load modeling during asymmetric disturbance in a metropolitan power grid', *IEEE Trans. Power Syst.*, 2009, **24**, (3), pp. 1191–1197

23 Ai, Q., Zhen, Z.-Y.: 'Distributed generation and smart grid' (Shanghai Jiao Tong University Press, Shanghai, 2013)

24 Kasem Alaboudy, A.H., Zeineldin, H.H., Kirtley, J.: 'Simple control strategy for inverter-based distributed generator to enhance microgrid stability in the presence of induction motor loads', *IET Gener. Transm. Distrib.*, 2013, **7**, (10), pp. 1155–1162

25 Keyhani, A.: 'Design of smart power grid renewable energy systems' (John Wiley & Sons, Inc., IEEE Publication, Hoboken, New Jersey, 2011)

26 He, R.-M., Ma, J., Hill, D.J.: 'Composite load modeling via measurement approach', *IEEE Trans. Power Syst.*, 2006, **21**, (2), pp. 663–672

27 Ai, Q.: 'Artificial intelligence of modern power system identification' (Shanghai Jiao Tong University Press, Shanghai, 2012)

28 Bai, X.-F., Jiang, G.-D.: 'Load modeling based on improved K-means clustering algorithm and its application', *Electr. Power Autom. Equip.*, 2010, **30**, (7), pp. 80–83

29 Yao, Y., Ai, Q., He, X., *et al.*: 'Further research on load modeling and parameter identification based on online measured data'. Proc. of IASTED Int. Conf., Banff, Canada, 2012, pp. 275–282

30 Yuan, R.-F., Ai, Q., He, X.: 'Research on dynamic load modelling based on power quality monitoring system', *IET Proc. Gener. Transm. Distrib.*, 2013, **7**, (1), pp. 46–51

31 Chen, D., Zhu, G.: 'An investigation on optimal load distribution of microgrids', *Autom. Electr. Power Syst.*, 2010, **34**, (20), pp. 45–49